Spectrochimica Acta Part A 79 (2011) 1520–1523

Contents lists available at ScienceDirect

Spectrochimica Acta Part A: Molecular and Biomolecular Spectroscopy

journal homepage: www.elsevier.com/locate/saa

Preparation, characterization and photoluminescence properties of BaB_2O_4: Eu^{3+} red phosphor

Jie Liu, Xiang-De Wang, Zhan-Chao Wu*, Shao-Ping Kuang*

Key Laboratory of Eco-chemical Engineering, Ministry of Education, College of Chemistry and Molecular Engineering, Qingdao University of Science and Technology, Qingdao 266042, PR China

ARTICLE INFO

Article history:
Received 8 March 2011
Received in revised form 9 May 2011
Accepted 11 May 2011

Keywords:
Red-emitting phosphor
XRD
Photoluminescence
Concentration quenching
Charge compensation

ABSTRACT

A new red emitting BaB_2O_4: Eu^{3+} phosphor was synthesized by solid-state reaction method. X-ray powder diffraction (XRD) analysis confirmed the monoclinic formation of BaB_2O_4. Field-emission scanning electron-microscopy (FE-SEM) observation indicated that the microstructure of the phosphor consisted of irregular grains with heavy agglomerate phenomena. Upon excitation with 394 nm light, the BaB_2O_4: Eu^{3+} phosphor shows bright red emissions with the highest photoluminescence (PL) intensity at 611 nm due to $^5D_0 \rightarrow {}^7F_2$ transitions of Eu^{3+} ions. The CIE chromaticity coordinates are calculated from the emission spectrum to be $x = 0.64$, $y = 0.35$. The effects of the Eu^{3+} concentration on the PL were investigated. The results showed that the optimum concentration of Eu^{3+} in BaB_2O_4 host is 6 mol% and the dipole–dipole interaction plays the major role in the mechanism of concentration quenching of Eu^{3+} in BaB_2O_4: Eu^{3+} phosphor. The effect of charge compensation on the emission intensity was also studied. The charge compensations of Li^+, Na^+ and K^+ anions all increased the luminescent intensity of BaB_2O_4: Eu^{3+}. K^+ anion gave the best improvement to enhance the intensity of the emission, indicating K^+ is the optimal charge compensator. All properties show that this phosphor could serve as a potential candidate for application as a red phosphor for NUV chip LED.

1. Introduction

White light-emitting diodes (WLED) have already been used widely in many areas and have several promising features such as high luminous efficiency, low power consumption, maintenance and environmental protection [1,2]. Near-ultraviolet (NUV) conversion is the most available method which can achieve WLED [3,4]. In this method, red/green/blue tricolor phosphors are pumped by NUV-InGaN chips (~400 nm) to generate white light. So phosphors play a crucial role in these solid-state lighting devices. However, the main tricolor phosphors for NUV InGaN-based LEDs are still some classical phosphor, such as $BaMgAl_{10}O_{17}$: Eu^{2+} for blue, ZnS: (Cu^+, Al^{3+}) for green, and Y_2O_2S: Eu^{3+} for red [5]. Especially, the efficiency of the Y_2O_2S: Eu^{3+} red phosphor is about eight times less than that of the blue and green phosphors. Furthermore, the sulfide-based phosphors have low chemical stabilities against strong irradiation from InGaN chip and cause some environmental problems both in preparation and in application as they contain toxic elements. Therefore, it is urgent to find novel red phosphors, which exhibit intense red emission with strong excitation band at around 400 nm for NUV LED chips. The red phosphor is also required to have high chemical stability and good chromaticity coordinates near the National Television Standard Committee (NTSC) standard values for red.

Borate is excellent matrices for Eu^{3+}-activated phosphors due to several advantages such as low synthetic temperature, high stability and high luminescence efficiency. During the past few years, a number of red-emitting borate phosphors have been synthesized and studied extensively which can be used for fabricating WLEDs [6–10]. In this paper, a new phosphor of Eu^{3+} doped monoclinic BaB_2O_4 is synthesized by solid stated method. The optimum Eu^{3+} doped concentration, the critical distance of the concentration quenching, the mechanism of concentration quenching, and effect of charge compensation on luminescence intensity are also investigated.

2. Experimental

2.1. Synthesis

A series samples, $Ba_{1-x}B_2O_4$: $Eu^{3+}{}_x$ ($x = 0.00$, 0.02, 0.04, 0.06, 0.08, 0.10) were synthesized by a conventional solid-state reaction technique. The appropriate amount of $BaCO_3$ (A.R. grade), H_3BO_3 (A.R. grade) and Eu_2O_3 (99.99%) were firstly ground, and

* Corresponding authors. Tel.: +86 532 84023653; fax: +86 532 84023927.
E-mail addresses: wuzhan_chao@163.com (Z.-C. Wu), qustksp@126.com (S.-P. Kuang).

1386-1425/$ – see front matter © 2011 Elsevier B.V. All rights reserved.
doi:10.1016/j.saa.2011.05.009

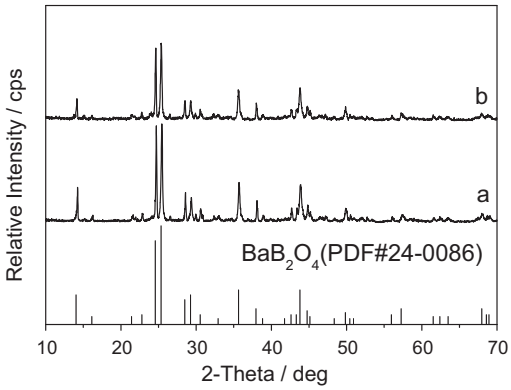

Fig. 1. XRD patterns of the samples (a: $Ba_{0.94}B_2O_4$: $Eu^{3+}{}_{0.06}$ and b: BaB_2O_4).

then burned in an electric furnace at 800 °C for 4 h. In some cases, appropriate amount of Li_2CO_3 (A.R. grade), Na_2CO_3 (A.R. grade) or K_2CO_3 (A.R. grade) were added as the charge compensators.

2.2. Measurements

Crystal phase identification was carried out on an X-ray diffractometer (D-MAX2500/PC, RIGAKU Corporation of Japan) using 40 kV, 20 mA, and Cu K_α radiation (1.5406 Å). Morphology and size of the calcined particles were observed by Field-emission scanning electron microscopy (FE-SEM, JSM-6700F, JEOL Corporation of Japan). Excitation and emission spectra of the powdered phosphors were measured on a Fluorolog-3-21 spectrometer (JOBIN YVON, America) and a 450 W xenon lamp was used as the excitation source. All measurements were made at room temperature unless otherwise stated.

3. Results and discussion

3.1. XRD of phosphor powders

The XRD patterns of the obtained BaB_2O_4 and $Ba_{0.94}B_2O_4$: $Eu^{3+}{}_{0.06}$ are given in Fig. 1. It can be found that the XRD patterns of BaB_2O_4 and $Ba_{0.94}B_2O_4$: $Eu^{3+}{}_{0.06}$ are consistent with JCPDS card (PDF#24-0086), indicating that doping of a small content of Eu^{3+} ion had little influence on the lattice structure of luminescence materials. The crystal structure of the prepared BaB_2O_4 can be refined to be monoclinic, space group *C2/c* with $a = 11.133$, $b = 12.67$ and $c = 8.381$. It is different from the reported β-BaB_2O_4, which is rhombohedral, space group *R3c* with $a = b = 12.532$ and $c = 12.726$ (PDF#38-0722) [10]. According to the calculated Hinckley index (crystallinity index) [11,12], $Ba_{0.94}B_2O_4$: $Eu^{3+}{}_{0.06}$ has a better crystallinity than BaB_2O_4.

3.2. FE-SEM images of phosphor powders

Fig. 2 shows the FE-SEM image of $Ba_{0.94}B_2O_4$: $Eu^{3+}{}_{0.06}$ powders prepared at 800 °C. It was observed that the microstructure of the phosphor consisted of irregular grains with heavy agglomerate phenomena. The average size of the $Ba_{0.94}B_2O_4$: $Eu^{3+}{}_{0.06}$ powders is about 2–6 μm. The results show that BaB_2O_4: Eu^{3+} phosphor has a good crystallinity and a relatively low sinter temperature, which is also consistent with the requirements of energy saving for products in today's society.

3.3. Photoluminescence properties

For the device application, overlap between the excitation spectra of phosphor and the emission spectrum of InGaN chip is required

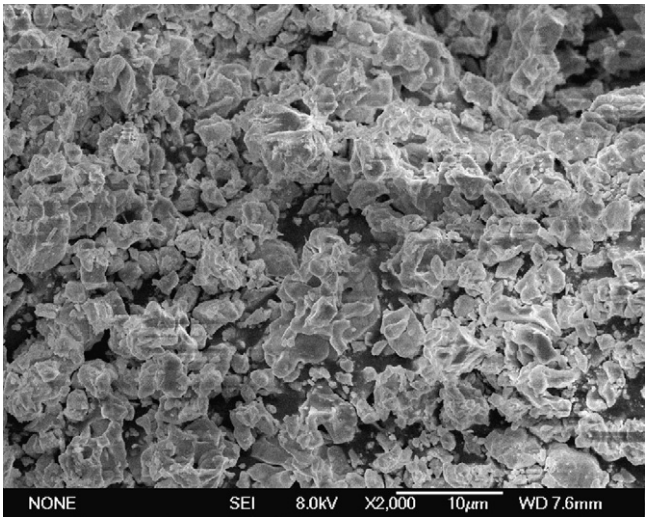

Fig. 2. FE-SEM images of $Ba_{0.94}B_2O_4$: $Eu^{3+}{}_{0.06}$.

to obtain high luminescence efficiency. The excitation (curve a) and emission (curve b) spectra of $Ba_{0.94}B_2O_4$: $Eu^{3+}{}_{0.06}$ are shown in Fig. 3. The broad excitation band at ~300 nm is attributed to the O → B charge transfer (CT) transition and the sharp lines in 360–480 nm range are intra-configurational 4*f*–4*f* transitions of Eu^{3+} in the host lattices. It is found that the excitation intensity at 394 nm is the highest in the excitation spectrum, which is attributed to the $^7F_0 \rightarrow {}^5L_6$ transition and matches the emission spectrum of the InGaN chip. The excitation peak at 465 nm is corresponding to the transition of $^7F_0 \rightarrow {}^5D_2$. The main emission peak in curve (b) is a $^5D_0 \rightarrow {}^7F_2$ transition of Eu^{3+} at 611 nm. Other transitions for the ^5D_J excited levels to ^7F_J ground states, such as $^5D_0 \rightarrow {}^7F_J$ lines in 570–720 nm range are relatively weak, which is advantageous to obtain the good CIE chromaticity coordinates. The results imply that Eu^{3+} ions occupy the lattice sites without inversion symmetry, which is in good agreement with the structural results. The CIE chromaticity coordinates are calculated from the emission spectrum to be $x = 0.64$, $y = 0.35$. Compared with the NTSC standard CIE chromaticity coordinate values for red ($x = 0.67$, $y = 0.33$), it is found that the CIE chromaticity coordinates of $Ba_{0.94}B_2O_4$: $Eu^{3+}{}_{0.06}$ are close to the NTSC standard values. These results imply that the luminescent property of $Ba_{0.94}B_2O_4$: $Eu^{3+}{}_{0.06}$ is good when it is applied in LED.

The effect of doped-Eu^{3+} concentration on the emission of BaB_2O_4: Eu^{3+} phosphor was also investigated. The emission spectra

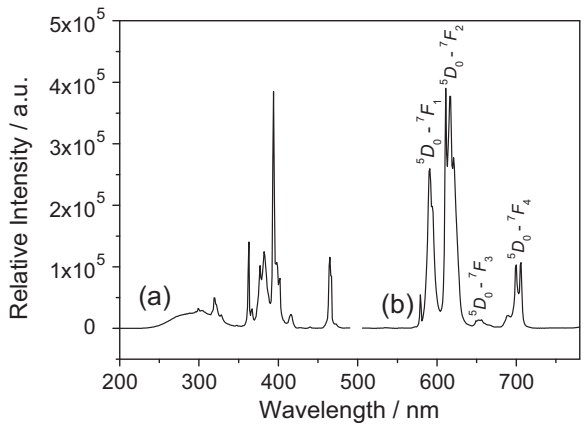

Fig. 3. Photoluminescence spectra of $Ba_{0.94}B_2O_4$: $Eu^{3+}{}_{0.06}$. (a) Excitation spectrum ($\lambda_{em} = 611$ nm) and (b) emission spectrum ($\lambda_{ex} = 394$ nm).

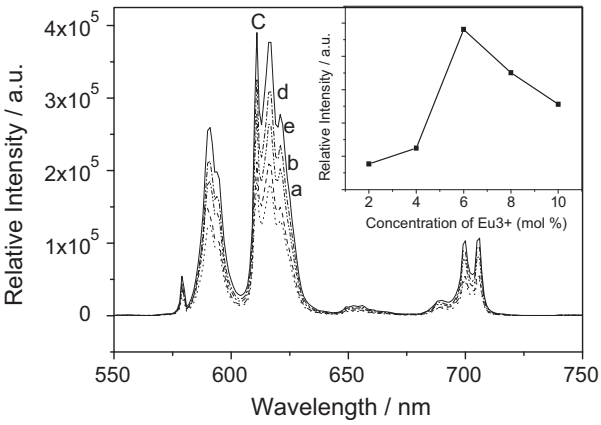

Fig. 4. Emission spectra of $Ba_{1-x}B_2O_4$: $Eu^{3+}{}_x$ with varying Eu^{3+} concentrations (a: $x = 0.02$, b: $x = 0.04$, c: $x = 0.06$, d: $x = 0.08$, and e: $x = 0.10$) ($\lambda_{ex} = 394$ nm). Inset: the dependence of PL intensity of $Ba_{1-x}B_2O_4$: $Eu^{3+}{}_x$ on Eu^{3+} concentration.

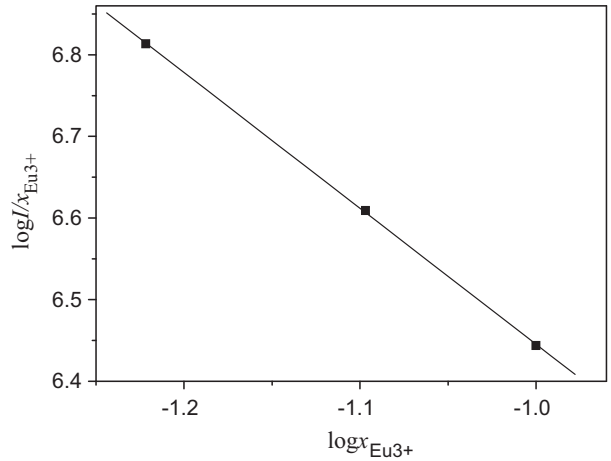

Fig. 5. The curve of $\log(I/\chi_{Eu^{3+}})$ vs. $\log(\chi_{Eu^{3+}})$ in $Ba_{1-x}B_2O_4$: $Eu^{3+}{}_x$ phosphor ($\lambda_{ex} = 394$ nm).

of BaB_2O_4: Eu^{3+} phosphors prepared at various concentrations of Eu^{3+} ($x = 0.02$–0.10) excited by 394 nm light and the dependence of photoluminescence (PL) intensity of $Ba_{1-x}B_2O_4$: $Eu^{3+}{}_x$ on doped-Eu^{3+} concentration are shown in Fig. 4. The PL intensity increases with Eu^{3+}-concentration increasing until a maximum intensity is reached, and then it decreases due to concentration quenching. The critical quenching concentration of Eu^{3+} (χ_c) is defined as the concentration at which the emission intensity begins to decrease and the critical distance is defined as the average distance between the nearest Eu^{3+} ions in which energy transfer occurs. From Fig. 4, we can see that χ_c of Eu^{3+} in BaB_2O_4: Eu^{3+} phosphor is about 6 mol%.

While discussing the mechanism of energy transfer in phosphors, Blasse [13] has pointed out that if the activator is introduced solely on Z ion sites, then there is on the average one activator ion per $V/\chi_c N$, where χ_c is the critical concentration, N is the number of Z ions in the unit cell, and V is the volume of the unit cell. The critical transfer distance (R_c) is approximately equal to twice the radius of a sphere with this volume.

$$R_c \approx 2\left(\frac{3V}{4\pi\ \chi_c N}\right)^{1/3} \quad (1)$$

By taking the values of $V = 1164.12$ Å^3, $N = 12$ and $\chi_c = 0.06$, the critical transfer distance of center Eu^{3+} in BaB_2O_4: Eu^{3+} phosphor is found to be 14.56 Å.

Non-radiative energy transfer between different Eu^{3+} ions may occur by exchange interaction, radiation re-absorption, or multipole–multipole interaction. Generally speaking, the mechanism of exchange interaction plays the role in energy transfer both when the overlapping of the wave functions of the sensitizer and activator is enough to exchange electronics and when the activator and sensitizer occupy adjacent lattice sites. Eu^{3+} is an isolated emission center in BaB_2O_4: Eu^{3+} phosphor and typical critical distance is then about 5 Å [14], which is far less than that of the sated calculation result of Eu^{3+}-doped in BaB_2O_4. This indicates that the mechanism of exchange interaction plays little role in energy transfer between Eu^{3+} ions in BaB_2O_4: Eu^{3+} phosphor. The mechanism of radiation re-absorption comes into effect only when there is a broad overlap of the fluorescent spectra of the sensitizer and activator, and in view of the emission and excitation spectra of BaB_2O_4: Eu^{3+} phosphor is unlikely to be occurring in this case. It is well known that the $^5D_0 \rightarrow {}^7F_2$ transition of Eu^{3+} is an electric-dipole transition, so the process of energy transfer should be controlled by electric multipole–multipole interaction according to Dexter's theory [14]. If the energy transfer occurs between the same sorts of activators, the intensity of multipolar interaction can be determined from the change of the emission intensity from the emitting level, which has the multipolar interaction. The emission intensity (I) per activator ion follows the equation [15–17],

$$\frac{I}{\chi} = K[1 + \beta(\chi)^{Q/3}]^{-1} \quad (2)$$

where x is the activator concentration; $Q = 6$, 8 or 10 for dipole–dipole, dipole–quadrupole or quadrupole–quadrupole interaction, respectively; and K and β are constants for the same excitation condition for a given host crystal.

Since the critical concentration of Eu^{3+} has been determined as 6 mol%, the dependence of the emission intensity of the BaB_2O_4: Eu^{3+} phosphor excited at 394 nm on the doped-Eu^{3+} concentration which is not less than the critical concentration (6 mol%) is determined (see Fig. 5). It can be seen from Fig. 5 that the dependence of $\log(I/\chi_{Eu^{3+}})$ on $\log(\chi_{Eu^{3+}})$ is linear and the slope is -1.67. The value of Q can be calculated as 5.01, which is approximately equal to 6, by using Eq. (2). This indicates that the dipole–dipole interaction is the major mechanism for concentration quenching of the central Eu^{3+} emission in BaB_2O_4: Eu^{3+}.

3.4. Effect of charge compensation on BaB_2O_4: Eu^{3+} luminescence intensity

In the BaB_2O_4: Eu^{3+} crystallite, Eu^{3+} is expected to replace Ba^{2+}. It would be difficult to keep the charge balance in the crystallite sample, so Eu^{3+} may not be fully introduced into the Ba^{2+} site. Consequently, univalent charge compensator (Li^+, Na^+ or K^+) was added as charge compensators in order to keep the charge balance. A series of $Ba_{0.88}M_{0.06}B_2O_4$: $Eu^{3+}{}_{0.06}$ (M = Li^+, Na^+ and K^+) samples and $Ba_{0.94}B_2O_4$: $Eu^{3+}{}_{0.06}$ were prepared. Their emission spectra, under excitation of 394 nm, are shown in Fig. 6. It is found that the charge compensations of Li^+, Na^+ and K^+ anions all increased the luminescent intensity of BaB_2O_4: Eu^{3+}. K^+ anion exhibits the strongest charge compensation abilities, Na^+ anion being the second, and Li^+ anion is the weakest. These phenomena are assigned to the fact that the ionic radius of K^+ (138 pm) is similar to that of Ba^{2+} (135 pm) so that K^+ can substitute Ba^{2+} easily without disturbing the crystal lattice. While there is a big discrepancy between the ionic radius of Na^+ (102 pm), Li^+ (59 pm) and Ba^{2+}, which leads to the different distortion grade of the crystal lattice and then impacts on the crystal structures and luminescent properties of phosphor [18]. Therefore, K^+ anion is the optimal charge compensator for BaB_2O_4: Eu^{3+}.

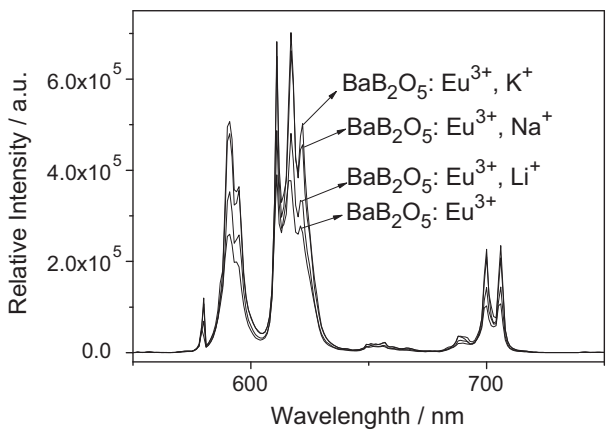

Fig. 6. Effect of different charge compensations on the emission intensity of BaB_2O_4: Eu^{3+}.

4. Conclusion

In this work, a new red-emitting phosphor of BaB_2O_4: Eu^{3+} was prepared by conventional solid-state reaction at 800 °C and its photoluminescence properties were investigated. It was found that the phosphor BaB_2O_4: Eu^{3+} exhibits efficient red-emitting at 394 nm excitation and appropriate CIE chromaticity coordinates ($x = 0.64$, $y = 0.35$). Based on the experimental results and the theoretical calculation, it is identified that the dipole–dipole interaction plays the major role in the mechanism of concentration quenching of Eu^{3+} in BaB_2O_4: Eu^{3+} phosphor. The charge compensations of Li^+, Na^+ and K^+ anions all increased the luminescent intensity of BaB_2O_4: Eu^{3+}. K^+ is the optimal charge compensator.

Acknowledgement

This work was financially supported by the National Natural Science Foundation of the People's Republic of China (Nos. 20977055, 21007029).

References

[1] S. Nakamura, S. Pearton, G. Fasol, The Blue Laser Diode, Springer, Berlin, 2000.
[2] Y.D. Huh, J.H. Shim, Y.R. Do, J. Electrochem. Soc. 150 (2003) H57–H60.
[3] Z.P. Yang, S.L. Wang, G.W. Yang, J. Tian, P.L. Li, X. Li, Mater. Lett. 61 (2007) 5258–5260.
[4] D. Jia, X.J. Wang, Opt. Mater. 30 (2007) 375–379.
[5] Z.L. Wang, H.B. Liang, M.L. Gong, Q. Su, Electrochem. Solid-State Lett. 8 (2005) H33–H35.
[6] X.M. Zhang, H.J. Seo, J. Alloys Compd. 503 (2010) L14–L17.
[7] N. Xie, Y.L. Huang, X.B. Qiao, L. Shi, H.J. Seo, Mater. Lett. 64 (2010) 1000–1002.
[8] W.R. Liu, C.C. Lin, Y.C. Chiu, Y.T. Yeh, S.M. Jang, R.S. Liu, Opt. Express 18 (2010) 2946–2951.
[9] P.L. Li, Z.J. Wang, Z.P. Yang, Q.L. Guo, G.S. Fu, Mater. Res. Bull. 44 (2009) 2068–2071.
[10] W.G. Zou, M.K. Lü, F. Gu, Z.L. Xiu, S.F. Wang, G.J. Zhou, Opt. Mater. 28 (2006) 988–991.
[11] D.N. Hinckley, Proceedings of the 11th National Conference of Clays and Clay Minerals, Pergamon, New York, 1963, pp. 229–235.
[12] J.H. Du, G. Morris, R.A. Pushkarova, R.S.C. Smart, Langmuir 26 (2010) 13227–13235.
[13] G. Blasse, Philips Res. Rep. 24 (1969) 131–144.
[14] D.L. Dexter, J. Chem. Phys. 21 (1953) 836–850.
[15] L.G. Van Uitert, J. Electrochem. Soc. 114 (1967) 1048–1053.
[16] L. Ozawa, P.M. Jaffe, J. Electrochem. Soc. 118 (1971) 1678–1679.
[17] Q.Z. Wang, J. Tian, X.H. Yang, X. Gao, J. Chin. Lumin. 16 (1995) 57–62.
[18] X. Li, Z.P. Yang, L. Guan, J.X. Guo, Y. Wang, Q.L. Guo, J. Alloys Compd. 478 (2009) 684–686.